

Aspect-Ratio Scaling and The Stiffness Exponent θ for Ising Spin Glasses

A. C. Carter, A. J. Bray, M. A. Moore

Department of Physics & Astronomy, The University of Manchester, Manchester M13 9PL, UK
(November 6, 2018)

We introduce the technique of *aspect-ratio scaling* to study the scale-dependence of interfacial energies in Ising spin glasses, and we show how one can use it to determine the stiffness exponent θ in a clean way, with results that are independent of the domain-wall-forcing boundary conditions imposed on the system. In space dimension $d = 2$ we obtain $\theta = -0.282(3)$ for a Gaussian distribution of exchange interactions.

The determination of stiffness exponents in spin glasses has a long history, going back to the early 1980s [1–3]. Loosely speaking, the stiffness exponent θ of an Ising spin-glass is defined by the statement that the energy, E_{int} , of an interface between ground states scales with length scale L as $E_{int} \sim L^\theta$. The looseness in this definition comes from the vagueness surrounding the phrase “length scale L ”. Since such interfaces are fractals [4,5], the length L does not refer to any measure on the interface itself, but rather to the size of the region in which the interface is confined. Traditionally, square or (hyper)cubic regions of side L are employed, with an interface imposed by a suitable change of boundary condition. The problem with this approach is that the results often seem to depend on the choice of boundary conditions. Here we explain why this is so and introduce the technique of *aspect-ratio scaling* as a method of obtaining a well-defined value for θ , independent of the boundary conditions imposed.

First we briefly review some of the different boundary conditions which have been used. For simplicity we discuss only space dimension $d = 2$, but generalization to $d > 2$ is trivial. In each case the boundary condition in the y -direction is periodic, while the domain-wall-forcing boundary conditions are imposed in the x -direction.

(i) *Periodic-Antiperiodic (P-AP)*: Ground state energies, E_P and E_{AP} , are determined for periodic and antiperiodic boundary conditions respectively (the latter often defined by reversing the signs of one column of bonds). The lower-energy state is obtained for **P** or **AP** boundary conditions with equal probability, and the higher-energy state contains a domain wall relative to the lower. The interface energy is therefore defined as $E_{int} = |E_P - E_{AP}|$.

(ii) *Free-Antifree (F-AF)*: The ground state energy, E_F , and spin configuration are obtained with free boundaries in the x -direction. The spins at one end are held fixed, those at the other end flipped, and the new ground state energy, E_{AF} , obtained. In this case $E_{int} = E_{AF} - E_F$, and $E_{int} > 0$.

(iii) *Random-Antirandom (R-AR)*: The spins at both ends are clamped in random configurations, and the ground-state energy, E_R , is obtained. The spins at one end are held fixed, those at the other end flipped, and the new ground-state energy, E_{AR} , is found. Now $E_{int} = |E_R - E_{AR}|$.

We now discuss the application of these methods to the nearest-neighbor Ising spin-glass model with Hamiltonian $H = -\sum_{\langle ij \rangle} J_{ij} S_i S_j$, restricting our attention initially to a Gaussian distribution of the exchange interactions, J_{ij} , in dimension $d = 2$. The **P-AP** method has traditionally been the most popular. The exponent θ has been measured for $d = 2$ [2,6], 3 [2,7] and 4 [8]. For $d = 2$ the result $\theta = -0.281(2)$ was obtained from square systems of size $L \leq 30$ [6]. A recent result by Hartmann and Young (HY) [9] on much larger square systems ($L \leq 480$), but using free boundaries in the y -direction, is consistent with this: $\theta = -0.282(2)$.

R-AR boundary conditions were used in early work by two of us [3] to obtain $\theta = -0.291(2)$ for $L \leq 12$. We believe (as will be discussed further below) that the small discrepancy with references [6,9] is due to the small range of sizes available in the earlier study.

Results for **F-AF** boundary conditions differ from the **P-AP** results by a somewhat larger amount, with $\theta = -0.20$ found for $L \leq 24$ [10], and $\theta = -0.266(2)$ obtained by HY using $L \leq 320$ (but with free boundaries in the y -direction). HY conjecture that the exponent is actually independent of the boundary conditions, but that larger sizes ($L \gg 320$!) are needed to reach the asymptotic regime for **F-AF** boundary conditions.

The questions raised by these results are (i) Are the results really boundary-condition-independent? If not, what does θ mean, and if θ is not well-defined, what are we to make of the conventional result $\xi \sim T^{1/\theta}$ [3] for the divergence of the correlation length as $T \rightarrow 0$? (ii) If θ *does* have a well-defined meaning, independent of the boundary conditions, is there an efficient method to obtain its asymptotic, boundary-condition-independent value?

To answer these questions we introduce here the idea of *aspect-ratio scaling* (ARS). Using this approach we obtain strong evidence for a unique θ , and we determine its value as $\theta = -0.282(3)$, consistent with values quoted above from studies using **P-AP** boundary conditions. For a given a number of spins, this approach apparently converges much more rapidly than using square samples.

Consider a system of length L and width M [11], where we will usually take $L \geq M$. The very natural assumption underlying ARS is that the mean interfacial energy (averaged over samples) has the asymptotic form (for L and M both large)

$$\langle E_{int} \rangle = M^\theta F\left(\frac{L}{M}\right) \quad (1)$$

where $L/M \equiv R$ is the aspect ratio of the samples. Now consider the limit $R \rightarrow \infty$. In this limit the system behaves like a $d = 1$ system, for which one can show that [3,13] $\langle E_{int} \rangle \sim 1/L$. Imposing this limiting form on (1) requires $F(x) \sim 1/x$ for $x \rightarrow \infty$, and gives

$$\langle E_{int} \rangle \sim \frac{M^{1+\theta}}{L}, \quad L \gg M. \quad (2)$$

It is also of interest to consider the limit $M \gg L$. In this limit, sections of the interface whose spatial extent is much larger than M are essentially independent, so we expect (for an $M^{d-1} \times L$ system) the M -dependence $\langle E_{int} \rangle \sim M^{(d-1)/2}$ for **P-AP** or **R-AR** boundary conditions, since the energies of different parts of the interface add with random signs, i.e. $F(x) \sim x^{\theta-(d-1)/2}$ for $x \rightarrow 0$ in (1), to give

$$\langle E_{int} \rangle \sim L^\theta \left(\frac{M}{L}\right)^{(d-1)/2}, \quad M \gg L \quad (\mathbf{P} - \mathbf{AP}, \mathbf{R} - \mathbf{AR}), \quad (3)$$

while for **F-AF** boundary conditions they will add with the same sign to give

$$\langle E_{int} \rangle \sim L^\theta \left(\frac{M}{L}\right)^{d-1}, \quad M \gg L \quad (\mathbf{F} - \mathbf{AF}). \quad (4)$$

Since the asymptotic forms (3) and (4) are different, it follows that the scaling function $F(x)$ in (1) will depend on the boundary conditions for general x . However, the limiting large- x form, which leads to (2), will be *independent* of the boundary conditions

If the limit $L \gg M$ can be achieved in practice, so that the form (2) holds, the exponent θ can be extracted from the M -dependence, and is transparently independent of the boundary conditions, i.e. if we define

$$G(M) = \lim_{L \rightarrow \infty} L \langle E_{int} \rangle, \quad (5)$$

then $G(M) \rightarrow AM^{1+\theta}$ for $M \rightarrow \infty$ ($A = \text{const.}$), giving

$$\theta = \lim_{M \rightarrow \infty} \frac{d \ln G}{d \ln M} - 1, \quad (6)$$

which is clearly independent of the boundary conditions imposed in the x -direction since the limit $L \rightarrow \infty$ is taken before the limit $M \rightarrow \infty$.

In practice we find it convenient to study a broad range of R rather than just the regime $R \gg 1$, though the exponent θ will ultimately be obtained by extrapolation to the $R = \infty$ limit. Figure 1 shows a log-log plot of $L \langle E_{int} \rangle$ against M for various fixed aspect ratios R ($1 \leq R \leq 32$), with **R-AR** boundary conditions. The ground state energies were obtained by using exact transfer matrix calculations, with $2 \leq M \leq 12$. Each point is an average of

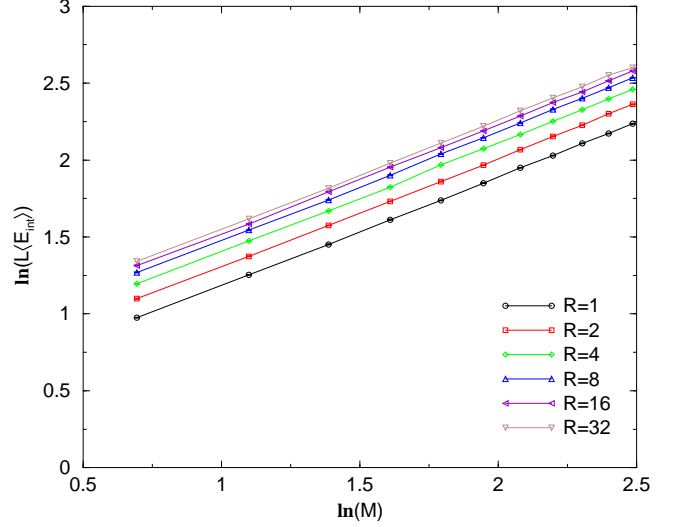


FIG. 1. Variation of $\langle E_{int} \rangle$ with width M at fixed R for **R-AR** boundary conditions.

10^5 samples. If ARS works perfectly for all L and M , the lines corresponding to different R will be parallel, with slope $1 + \theta$.

The lines are indeed almost straight and parallel. The slopes, θ_R ($R = \text{“random”}$) are presented for different aspect ratios in Table 1. The $R = 1$ result, corresponding to squares, is consistent with that obtained earlier using the same method [3]. However, there is a very slow decrease of the effective exponent with increasing R . We have argued that it is sensible to extract the exponent from the large- R limit, since in this limit any errors due to finite-size corrections in the x -direction are eliminated. Note that when the data are truly in the regime $R \gg 1$, the lines in Figure 1 will fall on top of each other. While they appear to be approaching a limit, they have not yet reached the limit at $R = 32$.

R	θ_R	θ_F
1	-0.289(2)	-0.153(2)
2	-0.286(2)	-0.215(2)
4	-0.285(2)	-0.249(2)
8	-0.283(2)	-0.265(2)
16	-0.285(2)	-0.273(2)
32	-0.283(2)	-0.274(3)

TABLE I. Effective stiffness exponent θ as a function of the aspect ratio R for **R-AR** (θ_R) and **F-AF** (θ_F) boundary conditions, obtained from gradients of the lines in figures 1 and 2.

The equivalent results for **F-AF** boundary conditions are presented in Figure 2. In this case the lines are clearly *not* parallel, i.e. there is a strong dependence of the measured gradients on R . The lines are also noticeably curved, especially for smaller values of R , e.g. for

$R = 1$ the slope (and therefore the effective value of θ) is decreasing with increasing M .

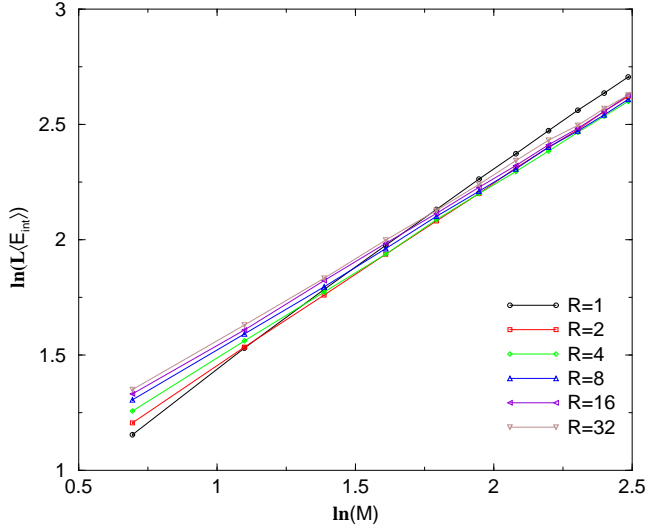


FIG. 2. Variation of $\langle E_{int} \rangle$ with width M at fixed R for F-AF boundary conditions.

Table 1 contains the effective exponents, θ_F ($F =$ “free”), extracted from Figure 2, for the different values of R . These exponents were obtained by fitting straight lines to the data, discarding the smallest value of M in each case. Note the strong dependence of θ_F on R . For $R = 1$ (i.e. squares) the effective θ_F differs by almost a factor 2 from the effective θ_R , but the difference gets smaller for larger values of R , and we argue that it approaches zero asymptotically. The argument is based on the following observation. For large R , we find that the interface energy is nearly always identical, sample by sample, for both boundary conditions. The differences apparent in Table 1 are due to a small fraction of the samples where the energies differ for the two boundary conditions. In fact, inspection of the interfaces themselves shows, as one would expect, that these occupy identical locations for the two boundary conditions whenever the interface energies are the same. To understand this we note the following facts:

(i) A detailed study of the ground states indicates that, for $R \gg 1$, the actual spin configurations are independent of the boundary conditions in the “interior” regions away from the boundaries. The effect of changing the boundary conditions is localized near the boundary, propagating a distance into the system whose mean size is roughly proportional to M over the range of M ($2 \leq M \leq 12$) studied.

(ii) The width of the interfacial region also scales roughly as M .

One can understand the latter as follows. Suppose this width scales as M^a . Then $a < 1$ would imply that the interface is “smooth” on large length scales, in-

consistent with it having a non-trivial fractal dimension $d_s > d - 1$. On the other hand, $a > 1$ would imply that for $M \gg 1$ the interface is strongly “stretched” in the x -direction. Its energy could then be estimated, using (3) with $M \rightarrow M^a$ and $L \rightarrow M$ as $E_{int} \sim M^{\theta+(a-1)(d-1)/2} \gg M^\theta$, which is inconsistent [12]. We conclude that $a = 1$. This means that there are of order $R = L/M$ independent places in which the interface can sit. Any one of these has an energy of order M^θ , but the prefactor is a random variable with non-zero weight at the origin [13]. The smallest of these therefore scales as $1/R$, i.e. $E_{int} \sim M^\theta/R$ for $R \gg 1$, a result identical to Eq. (2). From (i) and (ii) we see that the probability that the interface enters a region near the boundary where the ground-state spin configuration differs for the two sets of boundary conditions, and for which the interface energies also differ, is of order $1/R$ for large R .

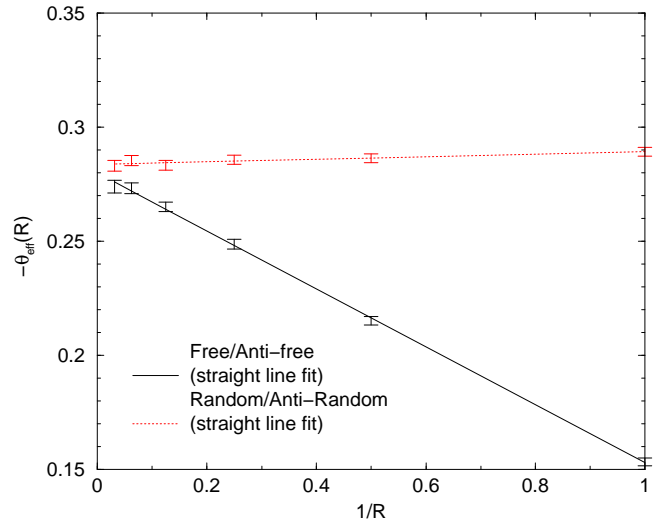


FIG. 3. Variation of θ_{eff} with system aspect ratio, R , for **R-AR** (upper data) and **F-AF** (lower data) boundary conditions. The data are consistent with convergence to a unique limiting value, $\theta = -0.282(3)$.

The above considerations suggest that convergence to the limiting behavior (2) occurs as $1/R$, so in Figure 3 we plot the effective exponents listed in Table 1 against $1/R$. The resulting plots are compatible with a linear dependence on $1/R$, and the data are consistent with convergence to a unique value, $\theta = -0.282(3)$, as $R \rightarrow \infty$.

It is remarkable that, by exploiting ARS, studies of systems with relatively small widths, $2 \leq M \leq 12$, can give results of comparable precision to studies on square systems of much larger size. This is especially striking for **F-AF** boundary conditions, where the effective exponent depends strongly on the aspect ratio R . For example, Table 1 shows that already for $R = 2$ the estimate of θ is more accurate than the result $\theta_F = -0.20$ obtained for

square systems of size up to 24 [10], while for $R = 8$ it matches the estimate $\theta_F = -0.266$ obtained from squares up to size 320 [9]. Furthermore, the ARS method demonstrates quite convincingly that the stiffness exponent is boundary-condition independent, a result which has not been confirmed conclusively for squares even on the largest systems studied [9]. This slow convergence of θ for **F- \mathbf{AF}** boundary conditions using squares suggests that other methods of determining θ , for example from the dependence on system size L of the Parisi overlap function $P(q)$ at $q = 0$ (notably in $d = 3$), using $P(0) \sim L^{-\theta}$, as predicted by the droplet model [4,13], or creating droplets by flipping a central spin while holding the boundary spins fixed [14], might also suffer from large finite-size effects.

We conclude by presenting some results for $d = 3$. The transfer matrix approach restricts us to rather small widths, $M \leq 4$. For each value of R we obtain an effective stiffness exponent θ_{eff} by fitting a straight line to the three points $M = 2, 3, 4$ in a plot of $\ln(L\langle|E|\rangle)$ against $\ln M$, and defining the slope to be $1 + \theta_{eff}$. These lines are found to be quite straight, so θ_{eff} can be readily extracted. It is plotted against $1/R$ in Figure 4, for both **R- \mathbf{AR}** and **F- \mathbf{AF}** boundary conditions. Also plotted are the equivalent results for the case where *free* boundaries are used in the directions normal to the domain-wall forcing boundary conditions. The final character in the legend specifies whether periodic (**P**) or free (**F**) boundaries have been employed in these directions. The free boundary data lie above the corresponding periodic boundary data in each case. The dependence of θ_{eff} on

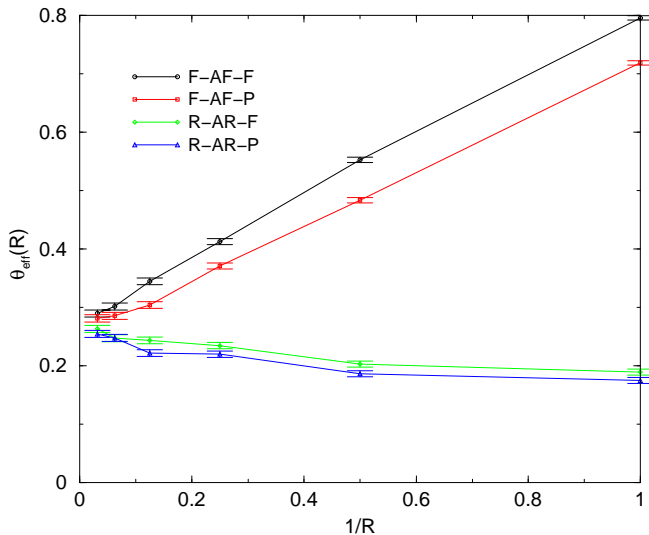


FIG. 4. Variation of θ_{eff} with system aspect ratio, R , in $d = 3$ for **R- \mathbf{AR}** (upper data) and **F- \mathbf{AF}** (lower data) boundary conditions. Periodic and free boundary conditions in the y direction are indicated by the final character **P** or **F**.

R in this case is quite striking. For **R- $\mathbf{AR-P}$** boundary

conditions, the $R = 1$ result, $\theta_{eff} \simeq 0.19$ is in agreement with our earlier results [3] on cubes of side $L = 2, 3, 4$ and those of Hartmann for $L \leq 10$ [7]. For $R \rightarrow \infty$, however, results for all boundary seem to converge to value $\theta \simeq 0.27$, significantly larger than previous estimates. It is surprising, also, that the boundary conditions in the transverse direction do not significantly affect the large- R limit of θ_{eff} . While the small widths M used prompts caution in the interpretation of this result (the same widths, used for $d = 2$, would give $\theta \simeq -0.32$ instead of -0.28), the trends with increasing R are quite striking. In particular, the use of **F- \mathbf{AF}** boundary conditions for cubes (i.e. $R = 1$) leads to a very large overestimate of the exponent.

In summary, the use of aspect-ratio scaling gives, in $d = 2$, results comparable in quality to those obtained from square systems of much larger size, and independent of the domain-wall-forcing boundary condition. It does this by eliminating finite-size corrections in the direction normal to the domain wall. For $d = 3$ the results suggest that θ may be significantly larger than previous estimates.

We thank A. P. Young for a useful discussion. This work was stimulated in part by comments from J. M. Kosterlitz concerning the possible influence of boundary conditions on the determination of stiffness exponents, and was supported by EPSRC.

-
- [1] J. R. Banavar and M. Cieplak, Phys. Rev. Lett. **48**, 832 (1982).
 - [2] W. L. McMillan, Phys. Rev. B **29**, 4026 (1984).
 - [3] A. J. Bray and M. A. Moore, J. Phys. C **17**, L463 (1984).
 - [4] D. S. Fisher and D. A. Huse, Phys. Rev. Lett. **56**, 1601 (1986); Phys. Rev. B **38**, 386 (1988).
 - [5] A. J. Bray and M. A. Moore, Phys. Rev. Lett. **58**, 57 (1987).
 - [6] H. Rieger, L. Santen, U. Blasum, M. Diehl, M. Junger, and G. Rinaldi, J. Phys. A **29**, 3939 (1996).
 - [7] A. K. Hartmann, Phys. Rev. E **59**, 84 (1999).
 - [8] A. K. Hartmann, Phys. Rev. E **60**, 5135 (1999).
 - [9] A. K. Hartmann and A. P. Young, preprint (condmat/0107308).
 - [10] F. Matsubara, T. Shirakura, and M. Shiomi, Phys. Rev. B **58**, R11821 (1998).
 - [11] This means $L \times M$ bonds, i.e. $(L + 1) \times M$ spins for **F- \mathbf{AF}** and **R- \mathbf{AR}** boundary conditions, and $L \times M$ spins for **P- \mathbf{AP}** boundary conditions.
 - [12] This argument, based on (3), is for **P- \mathbf{AP}** or **R- \mathbf{AR}** boundary conditions. For **F- \mathbf{AF}** boundary conditions an equivalent argument, based on (4), leads to the same conclusion.
 - [13] A. J. Bray and M. A. Moore, *Heidelberg Colloquium on Glassy Dynamics*, Lecture Notes in Physics **275**, 121 (Springer-Verlag, 1986).

[14] N. Kawashima, J. Phys. Soc. Jpn. **69**, 987 (2000).